Nuclear Magnetic Resonance and Crystallographic Studies of Chiral η^3-Allyl Palladium(II) Complexes and Asymmetric Allylic Alkylation of Propen-2-yl Acetates *

Edoardo Cesarotti,[a] Maria Grassi,[a] Laura Prati[a] and Francesco Demartin[b]

[a] *Università di Milano, Dipartimento di Chimica Inorganica e Metallorganica, Centro CNR, Via Venezian 21, I-20133 Milano, Italy*

[b] *Università di Milano, Istituto di Chimica Strutturistica Inorganica, Centro CNR, Via Venezian 21, I-20133 Milano, Italy*

The chiral complexes [Pd(η^3-allyl)(P–P')]X [P–P' = the chiral chelating ligand (*S*)(*N*-diphenylphosphino)(2-diphenylphosphinoxymethyl)pyrrolidine; allyl = MeCHCHCHMe, **2**; or PhCHCHCHPh **3**; X = BF_4^- or PF_6^-] have been prepared and analysed by NMR spectroscopy. Their diastereoisomeric composition have been determined on the basis of ^1H, ^{13}C, ^{31}P and two-dimensional ^1H–X (X = ^{13}C or ^{31}P) correlation NMR spectra. Since retention of the preferred *syn* disposition of the allylic substituents occurs in both cases the reaction product is a mixture of two isomers which differ in allylic chirality. The relative absolute configurations have been assigned by two-dimensional nuclear Overhauser effect measurements and confirmed by the X-ray crystallographic determination of the structure of the major diastereoisomer of **2**: the allyl fragments have (1*S*,3*R*) absolute configuration. The reaction of racemic 1,3-dimethylprop-2-enyl acetate in the presence of **2** and of 1,3-diphenylprop-2-enyl acetate in the presence of **3** with sodium dimethyl malonate gives the allylic alkylation products in 20 and 30% enantiomeric excess respectively.

The creation of stereocentres in high optical purity through the formation of carbon–carbon or carbon–heteroatom bonds is one of the most successful developments in the application of organometallic compounds to homogeneous catalysis; hydroformylation,[1] cyclopropanation,[2] aldol condensation[3] and allylic alkylation[4] are some examples of reactions catalysed by transition-metal complexes which have been transformed into stereocontrolled asymmetric syntheses with impressive success.

Allylic alkylation and related reactions have received great attention since the pioneering works of Tsuji,[5] Trost[6] and Kagan *et al.*[7] on palladium catalysts with chiral phosphines. Although many of the catalytic systems based on palladium diphosphine complexes have given excellent results, and despite the apparent simplicity of the proposed catalytic cycle, a general mechanism explaining the stereochemical outcome is still lacking. In these allylic alkylations the key intermediate is assumed to be a π-allyl–palladium(II) diphosphine complex which undergoes nucleophilic attack to give a palladium(0) phosphine, probably stabilized by a co-ordinated olefin. The zerovalent metal complex oxidatively adds the allylic substrate (usually an allyl acetate) to regenerate a π-allyl–palladium(II) intermediate. While a number of mechanistic studies and applications have been reported,[8] rarely has the structure of the intermediate been determined;[9] in particular, owing to the inherent complexity, no data exist about complexes where the chelating ligand does not have C_{2v} symmetry. However, a rationale for asymmetric allylic alkylations, comparable to that in the asymmetric catalytic hydrogenation of the precursors of amino acids with rhodium complexes,[10] requires a better knowledge of the structure of the intermediates and of the step determining the stereocontrol.

We have recently studied the stereochemistry in solution and the dynamic behaviour of [Pd(η^3-$CH_2CHMeCH_2$)(P–P')]$^+$ [P–P' = the chiral chelating ligand (*S*)(*N*-diphenylphosphino)(2-diphenylphosphinoxymethyl)pyrrolidine (dpopyr)][11,12] mainly by NMR spectroscopy, perhaps the most powerful method for structural investigations in chemistry and biochemistry upon the introduction of two-dimensional techniques.[13] In view of our interest in these above-mentioned areas we have extended this investigation to analogous diphosphine complexes bearing *meso* prochiral allyls.

Results and Discussion

The complexes are prepared as in equation (1). (R = Me, **2**; or

$$\tfrac{1}{2}[\{Pd(\eta^3\text{-RCHCHCHR})Cl\}_2] + AgX + dpopyr \longrightarrow [Pd(\eta^3\text{-RCHCHCHR})(dpopyr)]X + AgCl \quad (1)$$

Ph, **3**; X = BF_4^- or PF_6^-). Both **2** and **3** are stable white-yellow solids which slowly decompose in solution with separation of black material. They give satisfactory elemental analysis and have been fully characterized by multinuclear NMR (Tables 1 and 2) and mass spectroscopy. Slow recrystallization of **2** from methanol gives crystals suitable for X-ray diffraction study. Since the chiral phosphine has C_1 symmetry and the allyl bears substituents on terminal positions 1 and 3, complexes **2** and **3** might exist as eight diastereoisomers (Scheme 1).

The ^{31}P-{^1H} NMR spectra (Fig. 1) of the crude reaction mixture for both complexes **2** and **3** reveal that in **3** only two isomers are present and in **2** two species represent about 90% of the total amount (each diastereoisomer appears as a pair of doublets due to the presence of two different phosphorus atoms mutually coupled). The PO and PN assignment of resonances (Table 2) is made on the basis of literature[14] and confirmed by two-dimensional ^{31}P–^1H correlation NMR spectra.[11] Although fundamental for assignment purposes, the analysis of the corresponding ^1H NMR spectra (Fig. 2) is less simple due to the presence of significant numbers of diastereotopic protons in each isomer and the splitting of most of the resonances due to H–H and H–P couplings. As a consequence the complete

* *Supplementary data available:* see Instructions for Authors, *J. Chem. Soc., Dalton Trans.*, 1991, Issue 1, pp. xviii–xxii.

characterization of **2** and **3** requires a wide combination of one- and two-dimensional homo- and hetero-nuclear measurements. We limit our discussion to the findings which are significant for the determination of the diastereoisomeric composition. The relevant data are reported in Tables 1 and 2, and the labelling used for the ^1H and ^{13}C resonances is shown in Scheme 2; primed symbols in the text indicate the signals of a minor isomer.

In both cases we start from the ^{13}C NMR spectra. On the basis of *J*-modulation ^{13}C measurement and comparative analysis with the results for complex **1**[11] the phosphine and allylic resonances are clearly differentiated. The corresponding protons are identified straightforwardly by C–H correlation measurements. The method is especially useful in the recognition of the hidden ^1H allylic resonances of the minor isomers (b′,c′,e′; Table 1). Since all the allylic protons are mutually coupled, their connectivity is easily resolved by COSY-90 and COSY-LR measurements. For instance in the case of **2** the assignment of the central protons (e at δ 5.10 and e′ at δ 5.55) allows the relative allylic proton network to be clarified. Since the allylic ^3J(H–H) values are geometry dependent,[15,16] the analysis of the spin systems of **2** and **3** yields the stereochemistry.

By inspecting the cross-sections of the two-dimensional ^1H *J*-resolved spectra we observe that in both cases the central allylic protons e and e′ are triplets with ^3J(H–H) > 12 Hz

Table 1 Proton NMR data* for complexes **2** and **3**

Complex	a	b	c	d	e	H^2
2a	1.30	4.36 (11.4)	4.07 (13.0)	0.95	5.10	5.01
2b	1.45	3.15	3.5	0.95	5.55	4.70
3a	n.a.	5.7 (11.7)	5.2 (15.6)	n.a.	6.3	5.05
3b	n.a.	4.4	4.7	n.a.	6.9	4.55

* In $CDCl_3$, 298 K, at 200.13 MHz; chemical shifts (δ) referred to $SiMe_4$ with coupling constants (to ^{31}P) (in parentheses) in Hz. n.a. = Not assigned. In **2a** and **2b**, a = d = Me and b = c = e = H; in **3a** and **3b**, a = d = Ph and b = c = e = H.

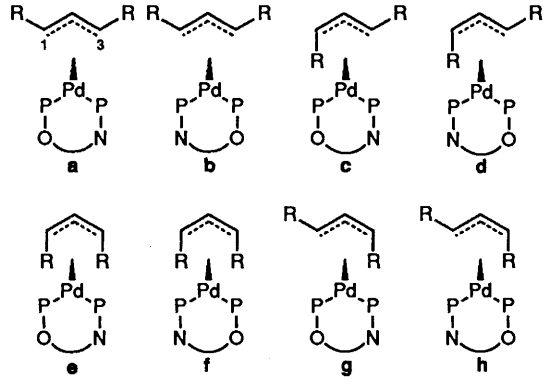

Scheme 1 Stereostructures of complexes **2** and **3**; carbon atoms 1 and 3 correspond to atoms C(2) and C(4) or C(7) and C(9) respectively of the two independent cations in the structure determination

Table 2 Carbon-13 and ^{31}P NMR data* for complexes **2** and **3**

Complex	C_a	C_b	C_c	PO	PN
2a	86.84 [28.8]	122.7 [7.9]	87.23 [32]	124.02 (69.4)	73.3
2b	84.1 [28.8]	122.4 [7.4]	88.4 [30.4]	127.0 (71.0)	75.6
3a	90.94 [26.1]	113.19 [7.55]	91.34 [29.5]	125.1 (85.1)	73.23
3b	90.05 [25.8]	112.66 [7.3]	92.1 [28.5]	127.6 (89.5)	75.7

* In $CDCl_3$, 298 K, at 50.323 (^{13}C) and 81.015 MHz (^{31}P). Chemical shifts (δ) referred to $SiMe_4$ (^{13}C) and external H_3PO_4 (^{31}P); coupling constants are in Hz, J(C–P) in square brackets, J(P–P) in parentheses.

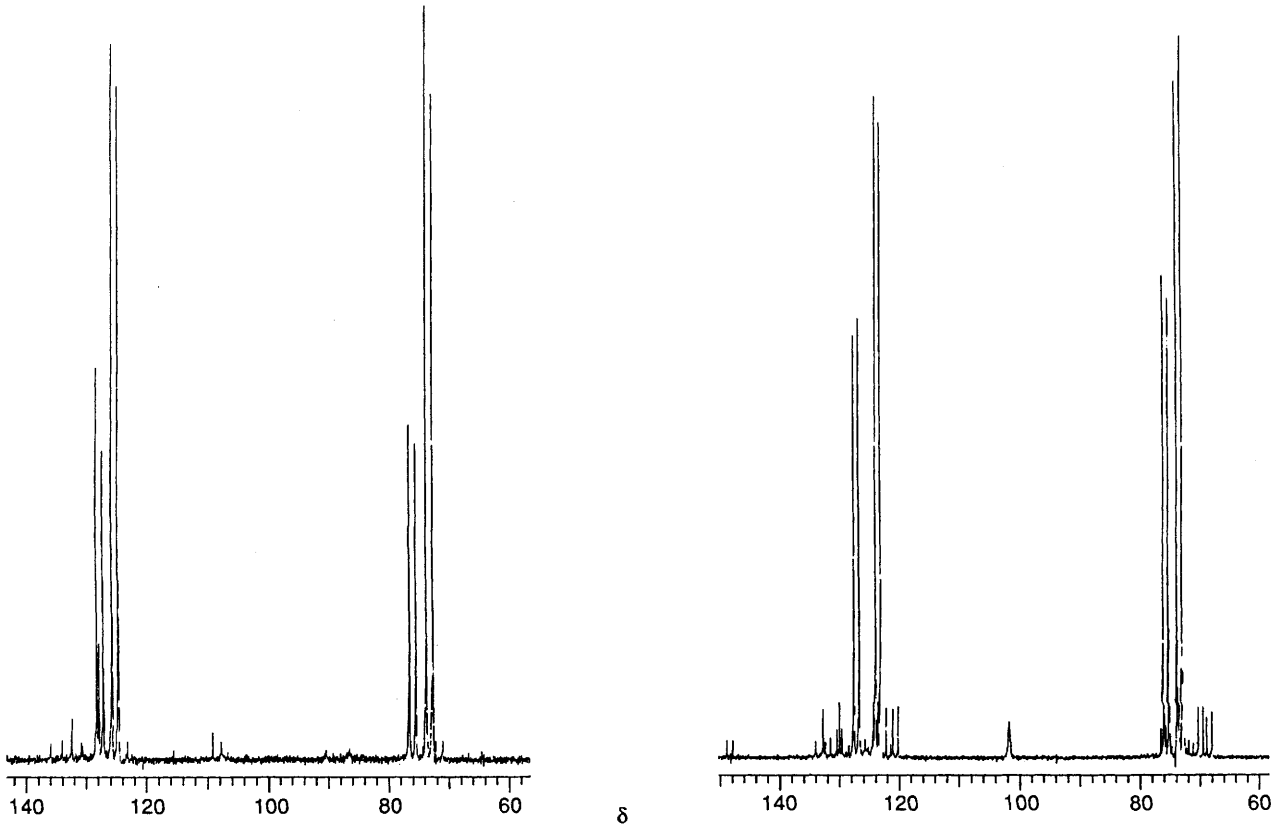

Fig. 1 The ^{31}P NMR (81.015 MHz, $CDCl_3$, 298 K) spectra of the crude reaction mixture of complexes **2** (right) and **3** (left)

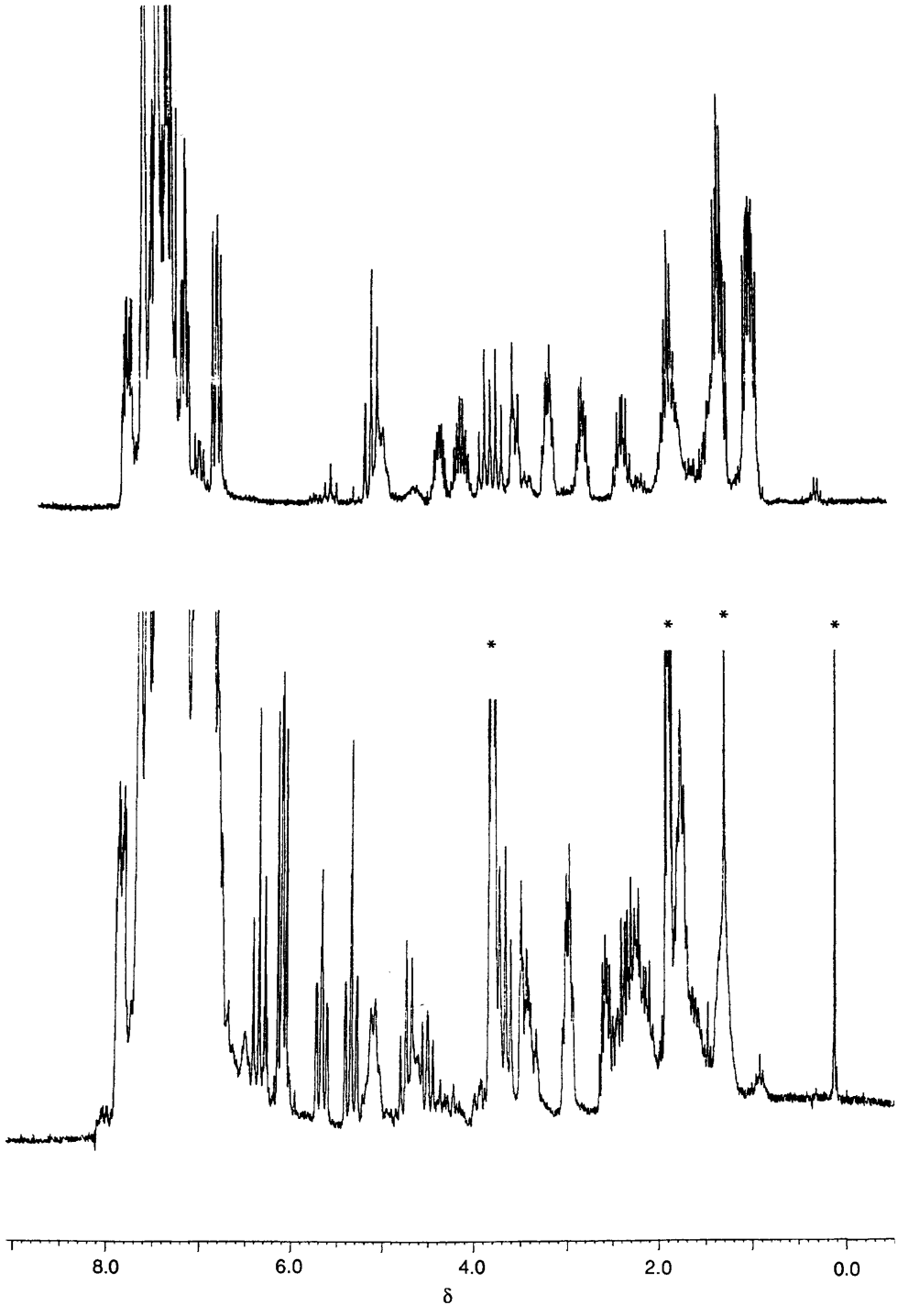

Fig. 2 Proton NMR (200.13 MHz, $CDCl_3$, 298 K) spectra of the crude reaction mixture of complexes **2** (above) and **3** (below). * Marks solvent peaks (thf) and impurities

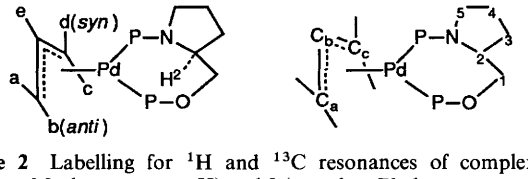

Scheme 2 Labelling for ^1H and ^{13}C resonances of complexes **2** (a = d = Me, b = c = e = H) and **3** (a = d = Ph, b = c = e = H)

which is typical for a *trans* H–H arrangement. Based on these data we can conclude that for complexes **2** and **3** the reaction product consists mainly of a mixture of diastereoisomers **a** and **b** of Scheme 1. Moreover analysis of the F2 projections of the *J*-resolution experiment allows determination of the ^1H–^{31}P couplings given in Table 1. Each individual ^1H resonance is associated with its corresponding ^{31}P absorption and the *cis*/*trans* arrangement of the allylic protons with respect to PO/PN is distinguished *via* ^1H–^{31}P correlation spectroscopy. In this methodology simplications occur in the ^1H spectrum since in the two-dimensional plot only the signals coupled to ^{31}P appear, further divided in rows pointing to the relative ^{31}P resonances. Fig. 3 shows the result of this measurement (performed in the inverse mode)[17] on complex **3**. It is known that in a co-ordinated allyl preferred coupling (through the metal) occurs between the *anti* protons and *trans* NMR-active nuclei (^{31}P in this case).[18] Thus a simple inspection of the horizontal rows (corresponding from top to bottom to PN, PN′, PO, PO′ resonances) leads to the following ^1H assignments: δ

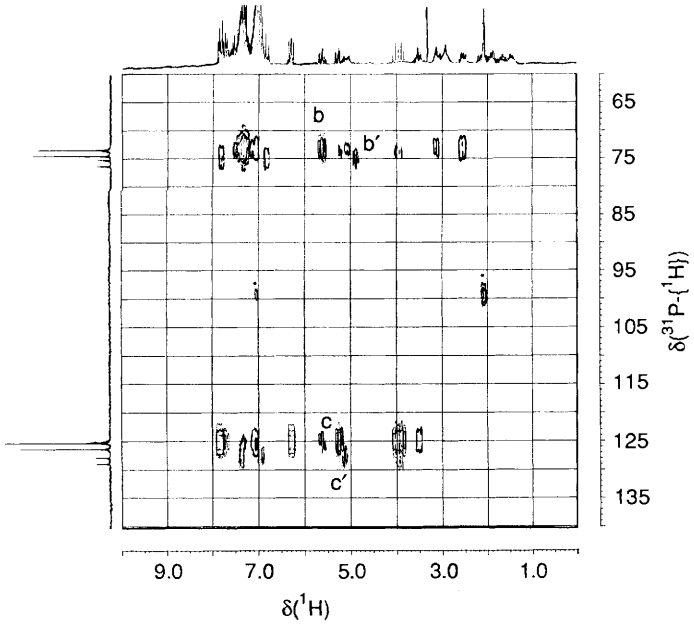

Fig. 3 Counter plot of the two-dimensional ^{31}P–^{1}H (200.13 MHz, CD_3COCD_3, 298 K) inverse correlation spectrum for complex **3**: b,c, and b′,c′ refer to the ^{1}H signals of the major and minor isomers respectively; * marks solvent peak and artefacts

5.75 (b), 4.85 (b′), 5.2 (c) and 5.13 (c′) (NB the slight variation in these data compared to the values in Table 1 is due to a solvent effect). Analogous information can be drawn from the ^{1}H NMR spectra measured under conditions of selective ^{31}P decoupling. The example given in Fig. 4 illustrates the results of these experiments on complex **2**. When PN and PO resonances are selectively irradiated decoupling is observed at δ 4.36 (b) and 4.07 (c) respectively. On the contrary, in both the experiments decoupling was observed at δ 1.3 (a) and 0.95 (d) thus indicating that $^{4}J(H\text{–}P_{trans})$ and $^{4}J(H\text{–}P_{cis})$ are of the same order of magnitude. Finally the ^{1}H-$\{^{31}P\}$ and ^{1}H–^{31}P correlation measurements allow some useful insight into the ^{1}H phenyl resonances. In particular the two sets of resolved signals at δ 7.8 and 6.8 (for **2**) and at 7.8 and 6.2 (for **3**) are assigned to the *ortho*-phenyl protons of the two rings bonded to PO (*i.e.* Ph_2 and Ph_1 respectively, see Scheme 3 and later).

The question of the absolute configuration of the major and minor diastereoisomers in **2** and **3** is settled by ^{1}H nuclear Overhauser effect (NOE) measurements. By inspecting the two-dimensional ^{1}H NOE spectra of the major isomers for both **2** and **3** the following observations can be made. (*i*) NOE is observed in both cases between the phenyl protons at δ 7.8 (Ph_2), the allylic *anti*-proton (b) and the proton H^2 of the co-ordinated ligand. (*ii*) NOE is also found for **2** between the ^{1}H phenyl at δ 6.8 (Ph_1), the *syn*-CH_3 at δ 1.3 and the central allylic proton (e) and for **3** between the ^{1}H phenyl at δ 6.2 and the central allylic proton (e). Overhauser factors vary with the internuclear distances (*r*) of the interacting nuclei as the inverse sixth power,[19] and usually no enhancement is observed for $r > 5$ Å. It is conceivable that the conformation of the co-ordinated ligand does not vary in the major and minor isomers, thus the relative stereostructures can be depicted as in Scheme 3. Considering the co-ordination plane (defined by PN–Pd–PO) our findings require that the phenyl ring at δ 7.8 (Ph_2), the *anti*-proton (b) and H^2 lie on the same hemispace, the phenyl ring at 6.8 or 6.2 (Ph_1) and the allylic proton (e) in the opposite. In other words for both **2** and **3** the major isomers have structure **a**. Whilst the absence of stereoisomers with allylic substituents in *anti* position (particularly for complex **3** bearing bulky phenyl groups on the allyl) is expected, the constant higher stability of structure **a** over **b** regardless of the nature of the allyl is rather remarkable.

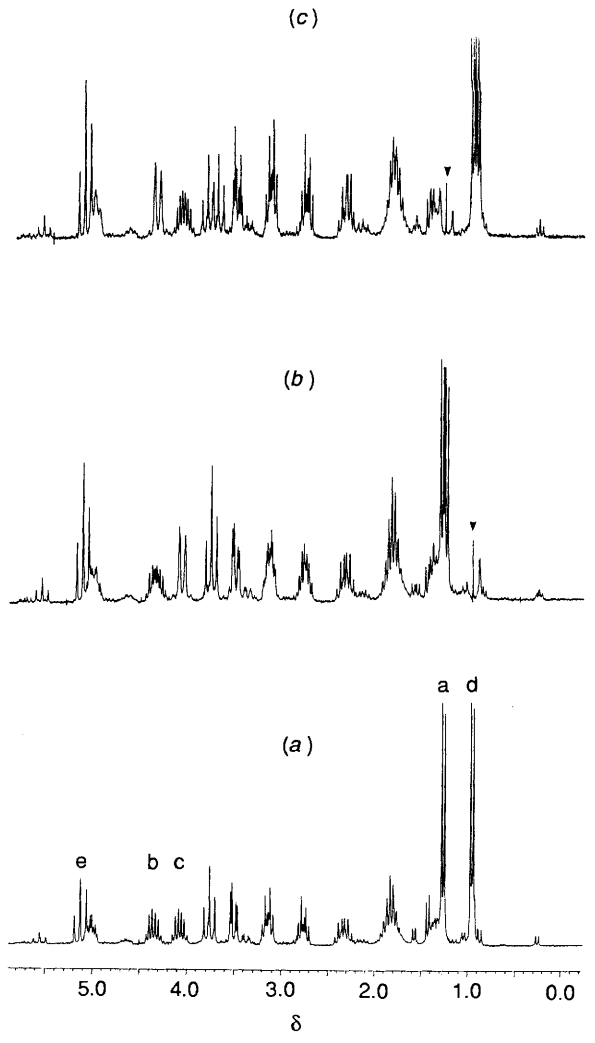

Fig. 4 Sections of the ^{1}H-$\{^{31}P\}$ decoupled (200.13 MHz, $CDCl_3$, 298 K) spectra for complex **2**: (*a*) BB ^{31}P decoupling at 81.023 MHz which corresponds to the middle of the ^{31}P spectrum; (*b*) ^{1}H decoupling at δ 0.95 (d) and simultaneous selective decoupling at 81.025 MHz (PO resonance); (*c*) ^{1}H decoupling at δ 1.30 (a) and simultaneous selective decoupling at 81.021 MHz (PN resonance); a–e refer to the allylic protons of the major isomer; (▼) resonances being saturated

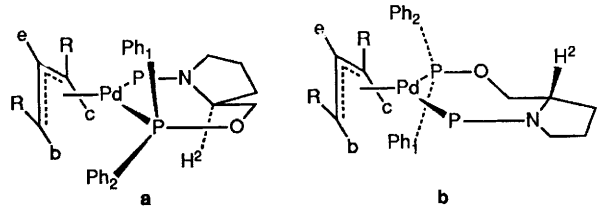

Scheme 3 Stereostructures of the major and minor isomers of complexes **2** and **3**

Similar results were obtained for [Pd(η^3-$CH_2CHMeCH_2$)-(dpopyr)] **1**[11] in which the allyl does not bear substituents in positions 1–3. This fact indicates that in the formation reaction of these complexes the stereo/electronic properties of the allyl play a minor role with respect to the chelating ligand. All the allyls examined have a *meso* structure, thus electronic effects from the chelating ligand are also excluded. We can conclude that the composition of the diastereoisomeric mixture of complexes **2** and **3** is under the steric control of the phosphine ligand. The presence of steric interaction between the phosphine and the co-ordinated allyl is further evidenced by the ^{1}H NMR findings (Table 1). Comparing the allylic resonances of the major and minor isomers we observe: (*i*) a shift to low field for

Table 3 Crystallographic data for [Pd(η³-MeCHCHCHMe)(dpopyr)]PF_6

Formula	$C_{34}H_{38}F_6NOP_3Pd$
M	790.00
Crystal system	Monoclinic
Space group	$P2_1$
a/Å	10.441(3)
b/Å	18.025(5)
c/Å	19.075(3)
β/°	96.52(2)
U/Å³	3567(3)
Z	4
F(000)	1608
D_c/g cm^{-3}	1.471
μ(Mo-Kα)/cm^{-1}	7.03
Minimum transmission factor	0.90
Scan mode	ω
ω-Scan width (°)	1.40 + 0.35tanθ
θ range (°)	3–25
Octants of reciprocal space explored	$\pm h, +k, +l$
Measured reflections	6678
Unique observed reflections with $I > 3\sigma(I)$	3207
Final R and R' [a]	0.067, 0.069
No. of variables	276
e.s.d. [b]	1.773

[a] $R = [\Sigma(F_o - k\|F_c\|)/\Sigma F_o]$, $R' = [\Sigma w(F_o - k\|F_c\|)^2/\Sigma w F_o^2]^{\frac{1}{2}}$. [b] e.s.d. = $[\Sigma w(F_o - k\|F_c\|)^2/(N_o - N_v)]^{\frac{1}{2}}$, where N_o, N_v = numbers of observations and variables.

both the *anti* protons (b,c compared to b′,c′); (*ii*) a shift to high field for the *syn* protons *cis* to PO and the central protons (a,e compared to a′,e′); (*iii*) no variation for the *syn* protons *cis* to PN (d compared to d′). These results, which fit well with the findings for **1**,[11] are explained on the basis of an anisotropic shielding effect from the phenyl rings of the phosphine on the allyl moiety. Moreover they require that the seven-membered ring formed by the ligand co-ordinated to Pd assumes a relatively rigid conformation thus creating a different chiral environment of the allyl in the two cases. A regular trend is also found for the ^{13}C and ^{31}P NMR data of all the complexes examined **1**–**3**. For example in the ^{31}P NMR spectra the resonances of **b** isomers are at higher fields and display larger homonuclear couplings than those of **a** isomers; in the ^{13}C NMR spectra always $\delta(C_c) > \delta(C_a)$ and $J(P\text{–}C_c) > J(P\text{–}C_a)$. All these data, although they do not explain the higher stability of isomers **a** over **b**, show that NMR spectroscopy affords an indication of the subtle structural differences for this class of compounds and allows a valuable insight into their stereochemistry in solution (not accessible by other means).

The dynamic behaviour of complexes **2** and **3** and the corresponding thermodynamic parameters has been studied on the basis of ^{31}P NMR results. In both cases the crude reaction mixture described in Fig. 1 does not represent the thermodynamic equilibrium and the quantitative analysis of ^{31}P NMR spectra reveals impurities arising from decomposition of the free ligand and of the complex. The low temperature spectrum in acetone at 203 K of a sample of **2**, purified from methanol, shows the presence of four isomers, of which **2a** comprises 85% of the total amount and the ratio **2a**/**2b** = 10.8:1. On raising the temperature only minor changes are observed but after a few hours at room temperature the spectrum indicates the presence of at least five isomers with **2a** comprising 77% of the total amount and **2a**/**2b** = 6.4:1. Since the same results, within the experimental error, have been obtained from a sample of **2** equilibrated at room temperature in $CDCl_3$ for 48 h (78% **2a**, **2b**/**2b** = 6.5:1) we can conclude that this represents the equilibrium ratio for complex **2**. These findings suggest that: (*a*) four-co-ordinate phosphine–allyl diastereoisomeric complexes with an *anti* disposition of the substituents are present in the thermodynamic mixture of **2** and (*b*) the overall isomerization process occurs very slowly. Accordingly negative results have been obtained in ^{31}P DANTE spin-saturation transfer and two-dimensional ^{31}P chemical exchange experiments. The isomerization of **2** occurs more rapidly in the presence of dpopyr. By adding a small amount (10%) of the phosphine ligand to many samples of **2** with diastereoisomeric composition ranging from pure **2a** up to a ratio **2a**/**2b** = 2:1, as in the crude reaction mixture, immediately the thermodynamic composition is observed. A DANTE spin-saturation transfer experiment provided evidence for dynamic exchange. Irradiation of the phosphorus signal at δ 123.7, corresponding to the higher frequency PO line of the isomer **2a**, leads to an excitation transfer to the signals at δ 129.4 and 122.0 due to two of the minor isomers of the thermodynamic mixture. It is widely accepted that allyl complexes can be dynamic through a π–σ–π process. Thus it is fairly likely that this mechanism applies also in the present case and that the minor isomers arise by *syn*/*anti* exchange of the allylic substituents at the 1 and 3 positions, although no other structural data are available about these less-abundant isomers. A slower dynamic process, not measurable by chemical exchange spectroscopy, equilibrates the isomers **2a** and **2b**. This is evidenced by the variation of their NMR ^{31}P absorptions (for example, **2a**/**2b** = 2:1 in the crude reaction mixture and 6.5:1 in the equilibrium mixture) and it is unambiguously demonstrated by the behaviour of the pure isomer **2a**. When a solution of the latter is treated with a small amount of the free phosphine ligand a rapid isomerization occurs giving rise to the equilibrium mixture; moreover this result helps to remove any ambiguity about the determination of the equilibrium conditions. When the equilibration is performed on samples of complex **2** with different diastereoisomeric compositions, owing to the presence of some decomposition, it is questionable whether the recorded spectrum represents the thermodynamic mixture or it is affected by different rates of decomposition of the isomers. On the contrary, no doubt is left when the equilibrium spectrum is observed starting from a sample of diastereoisomerically pure **2a**.

A rather different dynamic behaviour is observed for complex **3**. The low-temperature spectrum of a crystallized sample in acetone at 203 K shows the presence of almost pure isomer **3a**, isomer **3b** being less than 2%. After a few days at room temperature some changes are observed, the ratio **3a**/**3b** becoming 7:1. Since the same sample, kept at 0 °C for 6 months, gives an almost superimposable spectrum we may assume that this ratio represents the thermodynamic equilibrium. In an attempt to increase the isomerization rate, a small amount of phosphine was added to a solution of the crude reaction mixture and to a solution of diastereoisomerically pure **3a**. A change occurred immediately: the spectra of the two samples were almost identical showing the signals of the free phosphine ligand, the presence of some decomposition products and an isomer ratio **3a**/**3b** of *ca.* 20:1. This unexpected result can be explained by assuming that a new equilibrium point has been reached which accounts for the decomposition reaction of the isomers **3a**, **3b** and for the relatively newly formed species. In a similar reaction performed on complex **2** no change in the equilibrium ratio was observed thus indicating that the decomposition reactions of **2** can be ignored as far as the equlibration process is concerned. On the contrary, for complex **3**, the added free phosphine ligand might promote a faster decomposition of the minor isomer **3b** without further equilibration; equally the phosphine might stabilize isomer **3a** over **3b**. Since no free phosphine should usually be present in the catalytic allylation cycle a deeper understanding of this system, which would require a complex kinetic approach, is left to a subsequent paper.

Our NMR findings have been confirmed by the X-ray structure determination of suitable crystals of the major diastereoisomer of complex **2**, obtained after many efforts by slow recrystallization of the crude reaction mixture from methanol. Crystals of complex **2** contain discrete [Pd(η³-

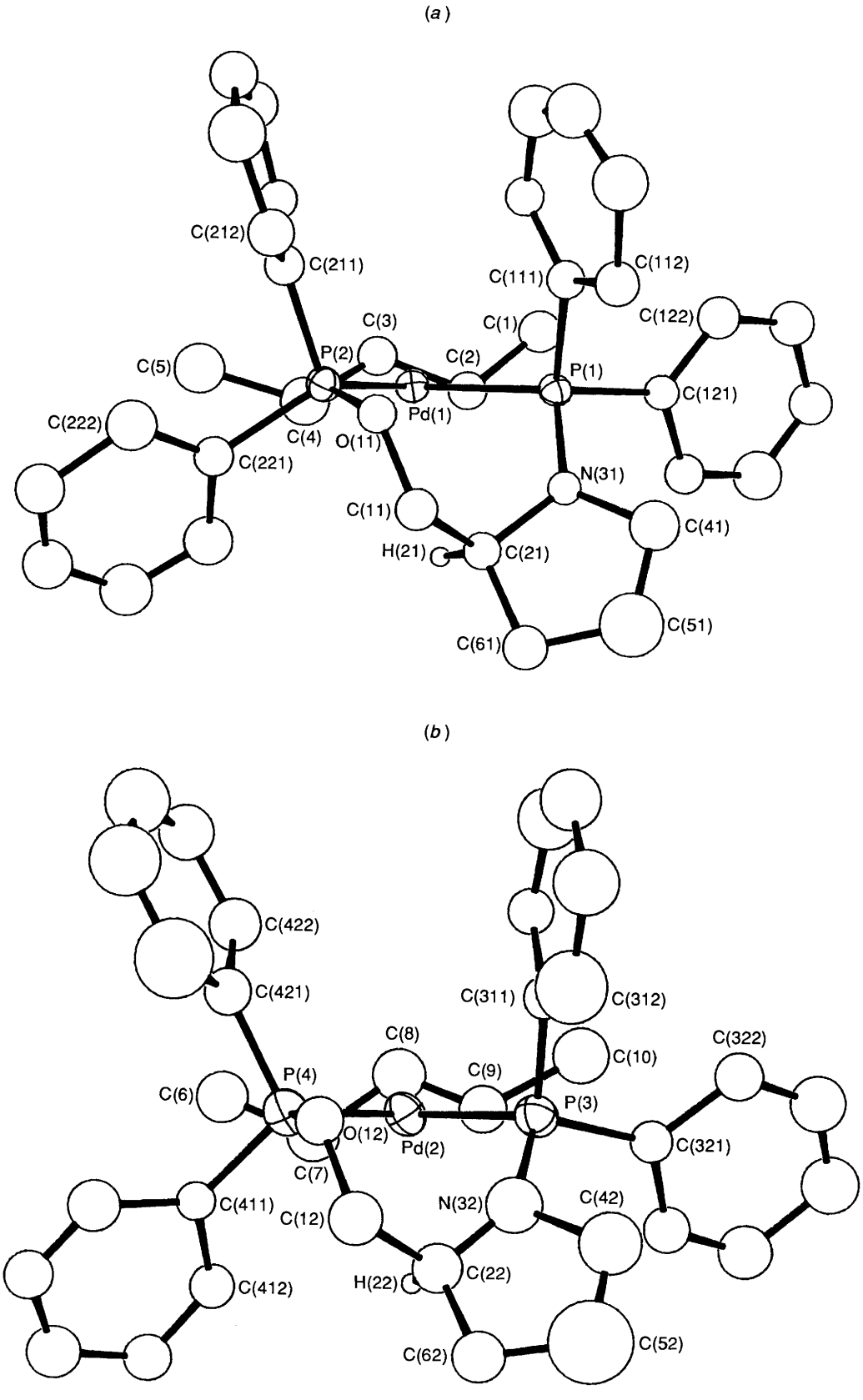

Fig. 5 ORTEP drawings of the two independent cations (*a*) and (*b*). Thermal ellipsoids drawn at 30% probability

MeCHCHCHMe)(dpopyr)]$^+$ cations and PF_6^- anions, packed with normal van der Waals contacts. The asymmetric unit in the space group $P2_1$ contains two independent cations, slightly differing in geometrical and conformational parameters as shown in Fig. 5(*a*) and (*b*) and two PF_6^- anions. As can be deduced from Table 3, the best crystals used for the structure determination are of poor quality (less than 50% of the collected reflections had $I \geqslant 3\sigma(I)$. During the structure solution some electron density close to one of the two independent cations could not be rationalized; as a consequence some anomalous bond distances

Table 4 Selected bond distances (Å), angles and torsion angles (°) with e.s.d.s in parentheses

Pd(1)–P(1)	2.300(4)	Pd(2)–P(3)	2.301(5)
Pd(1)–P(2)	2.276(4)	Pd(2)–P(4)	2.256(4)
Pd(1)–C(2)	2.27(2)	Pd(2)–C(7)	2.27(2)
Pd(1)–C(3)	2.24(2)	Pd(2)–C(8)	2.19(2)
Pd(1)–C(4)	2.17(2)	Pd(2)–C(9)	2.16(2)
P(1)–N(31)	1.69(1)	P(3)–N(32)	1.60(2)
N(31)–C(21)	1.46(2)	N(32)–C(22)	1.37(2)
C(21)–C(11)	1.52(2)	C(22)–C(12)	1.54(2)
C(11)–O(11)	1.44(2)	C(12)–O(12)	1.47(2)
O(11)–P(2)	1.61(1)	O(12)–P(4)	1.61(1)
N(31)–C(41)	1.43(2)	N(32)–C(42)	1.62(3)
C(41)–C(51)	1.43(3)	C(42)–C(52)	1.37(4)
C(51)–C(61)	1.49(3)	C(52)–C(62)	1.48(3)
C(61)–C(21)	1.51(2)	C(62)–C(22)	1.53(2)
P(1)–C(111)	1.84(2)	P(3)–C(311)	1.77(1)
P(1)–C(121)	1.83(1)	P(3)–C(321)	1.76(1)
P(2)–C(211)	1.79(2)	P(4)–C(411)	1.74(1)
P(2)–C(221)	1.82(2)	P(4)–C(421)	1.82(1)
C(1)–C(2)	1.48(2)	C(6)–C(7)	1.40(3)
C(2)–C(3)	1.39(2)	C(7)–C(8)	1.52(3)
C(3)–C(4)	1.41(2)	C(8)–C(9)	1.30(2)
C(4)–C(5)	1.59(2)	C(9)–C(10)	1.62(3)
P(5)–F(1–6) (average)	1.483	P(6)–F(7–12) (average)	1.517
P(1)–Pd(1)–P(2)	92.5(1)	P(3)–Pd(2)–P(4)	94.9(2)
C(2)–Pd(1)–C(3)	36.0(5)	C(7)–Pd(2)–C(8)	39.9(7)
C(3)–Pd(1)–C(4)	37.3(6)	C(8)–Pd(2)–C(9)	34.7(6)
C(2)–Pd(1)–C(4)	66.4(7)	C(7)–Pd(2)–C(9)	66.5(7)
Pd(1)–P(1)–N(31)	111.8(4)	Pd(2)–P(3)–N(32)	105.5(7)
P(1)–N(31)–C(21)	122.7(9)	P(3)–N(32)–C(22)	139(2)
N(31)–C(21)–C(11)	112(1)	N(32)–C(22)–C(12)	111(2)
C(21)–C(11)–O(11)	116(1)	C(22)–C(12)–O(12)	114(2)
C(11)–O(11)–P(2)	123(1)	C(12)–O(12)–P(4)	121(1)
O(11)–P(2)–Pd(1)	117.6(4)	O(12)–P(4)–Pd(2)	117.9(4)
C(21)–N(31)–C(41)	112(1)	C(22)–N(32)–C(42)	105(2)
N(31)–C(41)–C(51)	103(2)	N(32)–C(42)–C(52)	108(2)
C(41)–C(51)–C(61)	114(2)	C(42)–C(52)–C(62)	107(3)
C(51)–C(61)–C(21)	103(2)	C(52)–C(62)–C(22)	107(2)
C(61)–C(21)–N(31)	105(1)	C(62)–C(22)–N(32)	109(2)
C(11)–C(21)–C(61)	110(1)	C(12)–C(22)–C(62)	106(2)
C(1)–C(2)–C(3)	117(1)	C(6)–C(7)–C(8)	120(2)
C(2)–C(3)–C(4)	120(2)	C(7)–C(8)–C(9)	119(2)
C(3)–C(4)–C(5)	126(2)	C(8)–C(9)–C(10)	125(2)

Torsion angles within the seven-membered rings

Pd(1)–P(1)–N(31)–C(21)	−11.5(14)
P(1)–N(31)–C(21)–C(11)	−80.9(16)
N(31)–C(21)–C(11)–O(11)	57.2(20)
C(21)–C(11)–O(11)–P(2)	50.2(20)
C(11)–O(11)–P(2)–Pd(1)	−64.0(13)
O(11)–P(2)–Pd(1)–P(1)	−16.0(6)
P(2)–Pd(1)–P(1)–N(31)	59.4(5)
Pd(2)–P(3)–N(32)–C(22)	−9.7(29)
P(3)–N(32)–C(22)–C(12)	−78.8(31)
N(32)–C(22)–C(12)–O(12)	52.0(26)
C(22)–C(12)–O(12)–P(4)	48.3(23)
C(12)–O(12)–P(4)–Pd(2)	−73.1(15)
O(12)–P(4)–Pd(2)–P(3)	−4.4(7)
P(4)–Pd(2)–P(3)–N(32)	51.3(9)

are found and the molecular parameters, are affected by high estimated standard deviations (e.s.d.s) (see Table 4). Therefore a detailed discussion of the geometric features of the complex is prevented. Moreover the PF_6^- anions display quite 'lively' thermal parameters that probably are the result of the average of a slightly disordered situation that cannot be fitted by refining too close isotropic models. Nevertheless the structure determination of **2** allows us to establish unambiguously the configuration of the carbon atoms of the allyl group coordinated to palladium on the basis of the knowledge of the absolute configuration of the chiral centre of the diphosphine ligand [C(21) and C(22) in the two independent cations];[14] thus

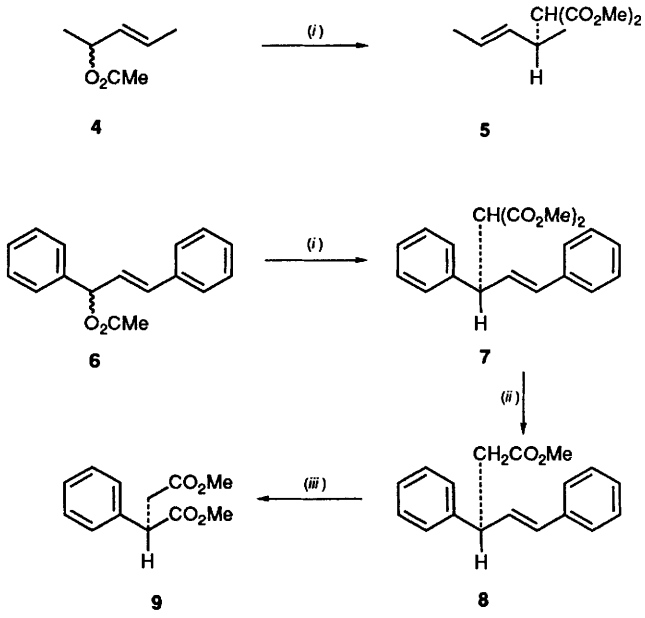

Scheme 4 Allylation of compounds **4** and **6** and decomposition of **7**. (*i*) Catalyst; (*ii*) NaCN, water, LiI, dmf; (*iii*) (*a*) O_3, (*b*) CH_2N_2

the allyl fragment in both the independent molecules has (1*S*) and (3*R*) absolute configuration. The ^{31}P NMR spectrum of the crystal used for the structure determination indicates that this is indeed the pure major component of the diastereoisomeric mixture of complex **2**.

Complexes **2** and **3** catalyse the addition of soft (carbon) nucleophiles to the corresponding allylic substrates; moreover they are assumed to be the key intermediates in the catalytic cycle originating in the oxidative addition of an allylic acetate to a [Pd°(P–P′)] complex. When racemic (*E*)-3-acetoxy-1,3-dimethylprop-1-ene **4** and (*E*)-3-acetoxy-1,3-diphenylprop-1-ene **6** are allowed to react with a 30% excess of sodium dimethyl malonate in the presence of 5 mol% of the corresponding allyl palladium dpopyr complex, dimethyl pent-3-en-2-ylmalonate **5** and dimethyl 1,3-diphenylprop-2-enylmalonate **7** are formed almost quantitatively (Scheme 4). The enantiomeric purities of **5** and **7** are estimated to be 20 and 30% enantiomeric excess (e.e.) respectively by ^1H NMR spectroscopy in the presence of the chiral shift reagent [Eu(hfc)$_3$]. Based upon the positive sign of the optical rotation it has been established that compound **5** has the *S* configuration.[20] The configuration of **7** is shown to be *R* by correlation to (*R*)-(−)-dimethyl phenylsuccinate **9** according to the sequence outlined in Scheme 4.

The enantioselectivity of the catalytic reaction is disappointingly low but the problem is whether or not it is possible to establish a correlation between the outcome of the catalysis and the observations on the dynamic behaviour of allylpalladium phosphine complexes in solution, this being the only way in which it is possible to define unambiguously how the chiral information located on the ligand is transferred to the substrates. The stereoelectronic properties of the allyl fragments cannot be taken into account in the explanation of the results of the allylation reaction because the *meso* nature of the allyls makes the two allylic termini equally probable for nucleophilic attack, in other words the enantioselectivity cannot be connected to a regioselectivity dictated by the nature of the allyl fragment. The electronic properties of the phosphine ligand also seem not to be determining because the NMR findings indicate that the chiral chelating ligand affects similarly complexes **2** and **3**, *i.e.* stabilizing structure **a** over **b** on the whole, and creating the same charge separation on the 1 and 3 allylic positions in the two complexes.

For complex **3**, in spite of the changes in the diastereoisomeric ratio with or without free phosphine ligand, no doubt exists that

structure **a** always largely prevails over **b** and no diastereoisomers with an *anti* disposition of the substituents are detectable. No definitive data are available about the diastereoisomeric ratio **3a**/**3b** in the presence of a nucleophile and the reactivity of each diastereoisomer, thus we cannot exclude that the stereoselectivity of the allylation might depend on the face selection of the allyl or on different reaction rates of the two diastereoisomers in respect of the nucleophile. With rather similar catalytic systems and substrates, Bosnich and his group[9] demonstrated that the turnover limiting step as well as the enantioselective step is the irreversible addition of the nucleophile to the four-co-ordinate phosphine–substrate diastereoisomers; it follows that the major diastereoisomeric allyl intermediate gives the lower-energy diastereoisomeric transition state and consequently the major enantiomer in the product. In that system however the substrates undergo attack exclusively at the less-substituted carbon atom of the allylic intermediate in the presence of a palladium phosphine catalyst. In our case an enantioselectivity of the allylation lower than the diastereoisomeric ratio is not surprising, provided that the regioselectivity of the nucleophilic attack is less than 100% directed toward one of the two allylic termini. Supposing that the stereochemistry of the allylation of compound **6** could be explained on the same thermodynamic and kinetic considerations as those invoked by Bosnich's group, the prevailing enantiomer **7** with an *R* configuration would be derived by preferential attack on the allyl carbon *trans* to PN in **3a** and *trans* to PO in diastereoisomer **3b**. If we consider now the allylation of **4** a striking contrast is evident: the prevailing enantiomer becomes **5** with an *S* configuration. If it would be possible to extend the same considerations invoked for the allylation of **6** to the reaction of **4**; as the diastereoisomer **2a** is always largely prevailing, the major enantiomer **5** should show the opposite *R* configuration. It is erroneous to draw any conclusion from this inversion of the overall stereochemistry of the catalytic reaction on moving from **4** to **6** but a simple inversion of the regioselectivity appears unlikely owing to the *meso* nature of the allyls and to the NMR findings which indicate a similar influence of the chiral chelating ligand on the complexes **2** and **3**. Another possible explanation may be a reversed reactivity on moving from catalyst **2** to **3**: in one catalytic system the diastereoisomers react at the same rate with the nucleophile; in the other catalytic system the minor diastereoisomer reacts faster than the major one. Alternatively one could assign to complex **2** a higher reactivity with the minor diastereoisomers which are very likely to have an *anti* disposition of the methyl groups, as has been shown recently in the allylation of η^3-allylpalladium 2,9-dimethyl-1,10-phenanthroline complexes.[21]

Asymmetric allylation is inherently a kinetic phenomenon and any rational development of these catalytic systems can be predicted only on a detailed knowledge of the mechanism and through the determination of the relative rates of the various steps. The interpretations of the results of the allylic substitution require however the acceptance that changes in the structure of the substrate involve a modification of the reaction profile making the allylation more similar to asymmetric hydrogenation in which it is now well established that the major product enantiomer originates in the minor four-co-ordinated diastereoisomer.[10] Kinetic experiments are in progress to elucidate the origin of such unexpected differences in stereoselectivity.

Experimental

The NMR measurements were made on Bruker AC-200 and Varian XL-200 spectrometers using standard[22] pulse sequences for *J*-modulation and two-dimensional experiments. A mixing time of 1 s was used in NOESY measurements. Inverse ^{31}P–^{1}H two-dimensional correlation (pulse sequence REVCORR from the Bruker library) and ^{1}H-{^{31}P} spectra were measured on a Bruker AC-200 instrument equipped with a second synthesizer for the X frequency generation (B-SV 3 unit); a 5 mm probe head with ^{1}H inner coil and tunable (BB) outer coil was employed. Solvents and temperatures are given in Tables 1 and 2.

The complexes were prepared under an atmosphere of dinitrogen, in solvents dried and degassed prior to use. Elemental analysis were performed at Dipartimento di Chimica Industriale ed Organica, Università di Milano. Mass spectra were recorded on a VG-7070 EQ mass spectrometer and the quoted M^+ was the peak in the parent multiplet which arose from the most abundant palladium isotope. The complexes [{Pd(η^3-allyl)Cl}$_2$] were prepared from $PdCl_2$ and allylic alcohols using literature methods.[9,15] Complexes **2** and **3** were prepared as described previously for **1**.[11] Satisfactory elemental analyses and fast atom bombardment (FAB) were obtained in both cases: [Pd(η^3-MeCHCHCHMe)(dpopyr)]BF_4 **2**, M^+ = 644 (Found: C, 51.50; H, 4.80; N, 1.70. Calc. for $C_{34}H_{38}BF_4NOP_2Pd$: C, 51.70; H, 4.80; N, 1.75%); [Pd(η^3-PhCHCHCHPh)(dpopyr)]BF_4 **3**, M^+ = 768 (Found: C, 62.40; H, 5.15; N, 1.10. Calc. for $C_{44}H_{42}BF_4NOP_2Pd$: C, 61.75; H, 5.15; N, 1.10%). The complex [Pd(η^3-MeCHCHCHMe)(dpopyr)]PF_6 for the X-ray structure determination was prepared in the same way as the BF_4^- salt using $AgPF_6$.

X-Ray Data Collection and Structure Determination.—Crystal data and other experimental details are summarized in Table 3. The diffraction experiment was carried out on a crystal with approximate dimensions 0.1 × 0.1 × 0.3 mm, using an Enraf-Nonius CAD-4 diffractometer at room temperature with graphite-monochromated Mo-Kα radiation (λ = 0.710 73 Å). The calculations were performed on a PDP11/73 computer using a SDP-Plus Structure Determination Package.[23] The diffracted intensities were corrected for Lorentz, polarization and absorption (empirical correction),[24] but not for extinction. Scattering factors for all atoms and anomalous dispersion corrections for scattering factors of non-hydrogen atoms were taken from ref. 25. The structure was solved by direct methods (MULTAN)[26] and refined by full-matrix least squares, minimizing the function $\Sigma w(F_o - k|F_c|)^2$. Weights assigned to individual observations were $w = 1/[\sigma(F_o)]^2$, where $\sigma(F_o) = [\sigma^2(I) + (0.04I)^2]^{\frac{1}{2}}/2F_oL_p$. Anistropic thermal factors were refined for Pd, P and F atoms. All the hydrogen atoms of the diphosphine ligand were introduced at calculated positions (C–H 0.95 Å) and not refined, while those belonging to the allylic moiety (not seen in a Fourier difference map) that cannot be unambiguously placed in calculated positions were omitted. The choice of the correct enantiomorph was made on the basis of previous knowledge of the absolute configuration of atoms C(21) and C(22) of the diphosphine ligand.[12,14] However a refinement of the other enantiomorph was tested but it was not significant, having afforded the same values of *R*, *R'* and goodness of fit for the correct enantiomer.

The final Fourier difference synthesis showed a maximum residual of 1.4 e Å^{-3} and some minor electron-density peaks close to one of the two independent cations with no clear significance. The atomic coordinates of the structural model are listed in Table 5.

Additional material available from the Cambridge Crystallographic Data Centre comprises H-atom coordinates, thermal parameters and remaining bond lengths and angles.

General Procedure for Allylic Alkylation.—A mineral oil dispersion of NaH (50% NaH, 2 g, 42 mmol) was washed free of paraffin with dry light petroleum and evaporated to dryness. The NaH was dissolved in MeOH (10 cm^3) and 1 equivalent of dimethyl malonate (5.54 g) added; the solution was stirred for 30 min and then evaporated leaving a white powder of sodium dimethyl malonate. The substrate (10 mmol) and catalyst (0.5 mmol) were dissolved in CH_2Cl_2 (10 cm^3) in a Schlenk tube provided with a serum cap under an inert atmosphere; sodium dimethyl malonate (13 mmol, 2 g) were dissolved in the

Table 5 Fractional atomic coordinates with e.s.d.s in parentheses

Atom	*x*	*y*	*z*	Atom	*x*	*y*	*z*
Pd(1)	1.364 6(1)	1.000	1.005 98(7)	C(113)	1.318(2)	1.231(1)	1.203(1)
Pd(2)	1.118 9(2)	0.796 0(1)	0.540 24(8)	C(114)	1.355(2)	1.272(1)	1.154(1)
P(1)	1.391 2(4)	1.023 5(3)	1.125 3(2)	C(115)	1.418(2)	1.246(1)	1.100(1)
P(2)	1.162 4(5)	1.048 9(3)	0.992 9(3)	C(116)	1.420(2)	1.172(1)	1.092(1)
P(3)	1.226 2(6)	0.723 0(3)	0.467 0(3)	C(121)	1.545(1)	0.996(1)	1.173 6(8)
P(4)	1.272 8(5)	0.787 6(4)	0.633 1(3)	C(122)	1.643(2)	1.044(1)	1.194(1)
P(5)	0.824 8(6)	0.588 9(4)	0.573 8(3)	C(123)	1.762(2)	1.020(1)	1.228(1)
P(6)	0.665 1(6)	0.225 6(4)	0.924 6(4)	C(124)	1.779(2)	0.947(1)	1.239(1)
F(1)	0.932(2)	0.560(1)	0.627(1)	C(125)	1.684(2)	0.900(1)	1.219(1)
F(2)	0.785(3)	0.634(2)	0.636(1)	C(126)	1.569(2)	0.922(1)	1.186(1)
F(3)	0.918(2)	0.646(1)	0.562 6(9)	C(211)	1.160(2)	1.143(1)	0.962(1)
F(4)	0.731(2)	0.621(1)	0.520(1)	C(212)	1.074(2)	1.194(1)	0.982(1)
F(5)	0.871(2)	0.546(1)	0.512(1)	C(213)	1.079(2)	1.266(1)	0.953(1)
F(6)	0.761(3)	0.520(1)	0.582(1)	C(214)	1.171(2)	1.286(1)	0.919(1)
F(7)	0.756(2)	0.287(1)	0.959(1)	C(215)	1.259(2)	1.238(1)	0.906(1)
F(8)	0.575(2)	0.166(1)	0.898(1)	C(216)	1.255(2)	1.165(1)	0.925(1)
F(9)	0.773(2)	0.199(1)	0.886(1)	C(221)	1.041(2)	1.002(1)	0.933 3(9)
F(10)	0.568(2)	0.261(1)	0.972(1)	C(222)	0.951(2)	1.040(1)	0.891(1)
F(11)	0.717(2)	0.177(1)	0.992(1)	C(223)	0.854(2)	0.998(2)	0.844(1)
F(12)	0.619(2)	0.276(1)	0.872(1)	C(224)	0.867(2)	0.928(1)	0.841(1)
O(11)	1.092(1)	1.060 6(7)	1.062 8(6)	C(225)	0.962(2)	0.889(1)	0.877(1)
O(12)	1.394(1)	0.734 1(8)	0.625 6(7)	C(226)	1.050(2)	0.924(1)	0.923(1)
N(31)	1.278(1)	0.980 0(7)	1.167 4(7)	C(311)	1.364(2)	0.770(1)	0.444(1)
N(32)	1.264(2)	0.649(1)	0.511(1)	C(312)	1.477(3)	0.735(2)	0.440(2)
C(1)	1.682(2)	0.976(1)	1.024(1)	C(313)	1.588(3)	0.777(2)	0.414(2)
C(2)	1.556(2)	0.945(1)	0.994(1)	C(314)	1.566(3)	0.851(2)	0.398(1)
C(3)	1.504(2)	0.973(1)	0.929(1)	C(315)	1.456(3)	0.883(2)	0.402(2)
C(4)	1.377(2)	0.955(1)	0.901(1)	C(316)	1.353(2)	0.846(1)	0.427(1)
C(5)	1.305(2)	0.984(1)	0.828(1)	C(321)	1.135(2)	0.695(1)	0.388(1)
C(6)	0.987(2)	0.910(1)	0.646(1)	C(322)	1.170(2)	0.710(1)	0.317(1)
C(7)	0.965(2)	0.856(1)	0.593(1)	C(323)	1.089(2)	0.687(2)	0.262(1)
C(8)	0.965(2)	0.878(1)	0.516(1)	C(324)	0.982(3)	0.649(2)	0.263(1)
C(9)	0.952(2)	0.826(1)	0.469(1)	C(325)	0.939(3)	0.634(2)	0.335(1)
C(10)	0.957(3)	0.840(2)	0.385(1)	C(326)	1.021(2)	0.653(1)	0.391(1)
C(11)	1.058(2)	1.000(1)	1.107 0(9)	C(411)	1.217(2)	0.761(1)	0.712(1)
C(12)	1.380(2)	0.653(1)	0.627(1)	C(412)	1.099(2)	0.723(1)	0.713(1)
C(21)	1.164(2)	0.945(1)	1.129 8(9)	C(413)	1.059(2)	0.699(1)	0.773(1)
C(22)	1.264(2)	0.623(1)	0.578(1)	C(414)	1.132(2)	0.711(1)	0.838(1)
C(41)	1.286(2)	0.969(1)	1.242(1)	C(415)	1.242(2)	0.747(1)	0.839(1)
C(42)	1.310(3)	0.579(2)	0.466(2)	C(416)	1.281(2)	0.771(1)	0.783(1)
C(51)	1.199(3)	0.909(2)	1.248(2)	C(421)	1.365(2)	0.873(1)	0.645(1)
C(52)	1.290(4)	0.516(3)	0.503(2)	C(422)	1.320(2)	0.938(1)	0.619(1)
C(61)	1.118(2)	0.890(1)	1.181(1)	C(423)	1.385(2)	1.006(2)	0.631(1)
C(62)	1.279(2)	0.538(1)	0.577(1)	C(424)	1.500(3)	1.005(2)	0.667(1)
C(111)	1.381(2)	1.124(1)	1.139(1)	C(425)	1.550(3)	0.944(2)	0.694(2)
C(112)	1.330(2)	1.149(1)	1.198(1)	C(426)	1.489(4)	0.873(2)	0.684(2)

minimum amount of CH_2Cl_2 and transferred with a syringe to the Schlenk tube and the reaction mixture was stirred for 15 h. After hydrolysis with aqueous acetic acid, the organic layer was separated, dried over Na_2SO_4 and evaporated *in vacuo*. The oily residue was purified by flash chromatography on silica gel [cyclohexane–ethyl acetate (5:1)]. Proton NMR ($CDCl_3$): dimethyl pent-3-en-2-ylmalonate **5**, δ 5.4 (m, 2 H), 3.7 (s, 6 H), 3.2 (d, 1 H), 2.7 (m, 1 H), 1.6 (d, 3 H) and 1.0 (d, 3 H); dimethyl 1,3-diphenylpropen-2-ylmalonate **7**, δ 7.0 (m, 10 H), 6.3 (m, 2 H), 4.13 (m, 2 H), 3.6 (s, 3 H) and 3.4 (s, 3 H).

Dimethyl Phenylsuccinate.—Compound **7** (100 mg, 0.3 mmol), dry LiI (200 mg, 1.5 mmol) and anhydrous NaCN (74 mg, 1.5 mmol) were dissolved in dimethylformamide (dmf) (5 cm^3) under nitrogen and heated at 120 °C for 24 h. The solution was poured into water (25 cm^3), the pH adjusted to 11 with aqueous NaOH and extracted with diethyl ether (3 × 25 cm^3). The combined organic extracts were dried and evaporated to an oil. The crude material was dissolved in CH_2Cl_2 (5 cm^3) and EtOH (5 cm^3) and ozonized at −70 °C for 120 min. The solvent was evaporated to a pale yellow oil which was treated with formic acid (3 cm^3, 90%) and H_2O_2 (1 cm^3, 36%). After 30 min the solution was heated at 120 °C in an oil-bath for 1 h. The solution was diluted with water (5 cm^3) and extracted with ether (3 × 10 cm^3). The combined ether extracts were dried over Na_2SO_4 and an ether solution of diazomethane, generated from Diazald (3 g), was distilled directly into the ether solution. After 2 h the solution was washed with water, dried over Na_2SO_4, and evaporated to leave an oily solid. Flash chromatography on silica gel [cyclohexane–ethyl acetate (5:1)] afforded dimethyl phenylsucciniate **9** (25 mg). Proton NMR ($CDCl_3$): δ 7.2 (s, 5 H), 4.1 (m, 1 H), 3.7 (s, 6 H) and 3.3 (m, 2 H). The compound showed a negative sign of optical rotation ($CHCl_3$).

Acknowledgements

We thank the Ministero per l'Università e la Ricerca Scientifica e Tecnologica for financial support.

References

1 G. Parrinello and J. K. Stille, *J. Am. Chem. Soc.*, 1987, **109**, 7122.
2 H. Fritschi, U. Leutenegger and A. Pfaltz, *Angew. Chem., Int. Ed. Engl.*, 1986, **25**, 1005.
3 Y. Ito, M. Sawamura, M. Kobayashi and T. Hayashi, *Tetrahedron Lett.*, 1988, 6321.

4 B. Bosnich and P. B. Mackenzie, *Pure Appl. Chem.*, 1982, **54**, 189.
5 J. Tsuji, *Acc. Chem. Res.*, 1969, **2**, 144.
6 B. M. Trost, *Acc. Chem. Res.*, 1980, **13**, 385.
7 H. B. Kagan, J. C. Fiaud, A. H. de Gournay and M. Larcheveque, *J. Organomet. Chem.*, 1978, **154**, 175.
8 G. Consiglio and R. N. W. Waymouth, *Chem. Rev.*, 1989, **89**, 257, and refs. therein; S. L. Blystone, *Chem. Rev.*, 1989, **89**, 1663 and refs. therein.
9 P. R. Auburn, P. B. Makenzie and B. Bosnich, *J. Am. Chem. Soc.*, 1985, **107**, 2033; P. B. Mackenzie, J. Whelan and B. Bosnich, *J. Am. Chem. Soc.*, 1985, **107**, 2046; J. M. Brown and J. E. Macintyre, *J. Chem. Soc., Perkin Trans. 2*, 1985, 961.
10 C. R. Landis and J. Halpern, *J. Am. Chem. Soc.*, 1987, **109**, 1746; P. L. Evans and J. M. Brown, *Tetrahedron*, 1988, **44**, 4905.
11 E. Cesarotti, M. Grassi and L. Prati, *J. Chem. Soc., Dalton Trans.*, 1989, 161.
12 E. Cesarotti, M. Grassi, L. Prati and F. Demartin, *J. Organomet. Chem.*, 1989, **370**, 407.
13 J. Schraml and J. M. Bellama, in *Two Dimensional NMR Spectroscopy*, Wiley, New York, 1988; K. Nagayama, in *NMR in Stereochemical Analysis*, VCH, Deerfield Beach, FL, 1986, vol. 6, ch. 5; A. E. Derome, in *Modern NMR Techniques for Chemistry Research*, Pergamon, Oxford, 1987.
14 E. Cesarotti, A. Chiesa, G. Ciani and A. Sironi, *J. Organomet. Chem.*, 1983, **251**, 79.
15 P. M. Maitlis, P. Espinet and M. H. Russel, in *Comprehensive Organometallic Chemistry*, Pergamon, Oxford, 1982, vol. 6, 410 and refs. therein.
16 A. T. Tayim and J. C. Bailar, *J. Am. Chem. Soc.*, 1967, **89**, 3420; H. C. Clark, C. Billard and C. S. Kong, *J. Organomet. Chem.*, 1980, **190**, 105.
17 H. Kessler, M. Gehrke and G. Griesinger, *Angew. Chem., Int. Ed. Engl.*, 1988, **27**, 490 and refs. therein; R. Benn and C. Brevard, *J. Am. Chem. Soc.*, 1986, **108**, 5622; A. Bax and S. Subramanian, *J. Magn. Reson.*, 1986, **67**, 565.
18 G. Carturan, A. Scrivanti, B. Longato and F. Morandini, *J. Organomet. Chem.*, 1979, **172**, 91; K. H. A. Ostoja Starzewski and P. S. Pregosin, *Adv. Chem. Ser.*, 1982, **176**, 23.
19 J. H. Noggle and R. E. Schirmer, in *The Nuclear Overhauser Effect*, Academic Press, New York, 1971.
20 B. M. Trost and T. J. Dietsche, *J. Am. Chem. Soc.*, 1973, **95**, 8200.
21 B. Åkermark, S. Hansson and A. Vitagliano, *J. Am. Chem. Soc.*, 1990, **112**, 4587.
22 R. Benn and H. Gunther, *Angew. Chem., Int. Ed. Engl.*, 1983, **22**, 350; G. A. Morris, *Magn. Reson. Chem.*, 1986, **24**, 371.
23 B. A. Frenz and Associates, SDP Plus Version 1.0, Enraf-Nonius, Delft, 1980.
24 A. C. North, D. C. Phillips and F. S. Mathews, *Acta Crystallogr., Sect. A*, 1968, **24**, 351.
25 *International Tables for X-Ray Crystallography*, Kynoch Press, Birmingham, 1974, vol. 4.
26 G. Germain, P. Main and M. N. Woolfson, *Acta Crystallogr., Sect. A*, 1971, **27**, 368.

Received 25*th February* 1991; *Paper* 1/00892G